# FGF-2–dependent signaling activated in aged human skeletal muscle promotes intramuscular adipogenesis

Sebastian Mathes[a,b], Alexandra Fahrner[a,b], Umesh Ghoshdastider[c], Hannes A. Rüdiger[d], Michael Leunig[d], Christian Wolfrum[c], and Jan Krützfeldt[a,b,1]

[a]Division of Endocrinology, Diabetes, and Clinical Nutrition, University Hospital Zurich, 8091 Zurich, Switzerland; [b]Biomedicine, Life Science Zurich Graduate School, University of Zurich, 8057 Zurich, Switzerland; [c]Institute of Food, Nutrition and Health, Department of Health Sciences and Technology, Eidgenössische Technische Hochschule Zurich, 8092 Zurich, Switzerland; and [d]Department of Orthopaedics, Schulthess Clinic, 8008 Zurich, Switzerland

Edited by Ronald M. Evans, Salk Institute for Biological Studies, La Jolla, CA, and approved June 23, 2021 (received for review October 13, 2020)

**Aged skeletal muscle is markedly affected by fatty muscle infiltration, and strategies to reduce the occurrence of intramuscular adipocytes are urgently needed. Here, we show that fibroblast growth factor-2 (FGF-2) not only stimulates muscle growth but also promotes intramuscular adipogenesis. Using multiple screening assays upstream and downstream of microRNA (miR)-29a signaling, we located the secreted protein and adipogenic inhibitor SPARC to an FGF-2 signaling pathway that is conserved between skeletal muscle cells from mice and humans and that is activated in skeletal muscle of aged mice and humans. FGF-2 induces the miR-29a/SPARC axis through transcriptional activation of FRA-1, which binds and activates an evolutionary conserved AP-1 site element proximal in the miR-29a promoter. Genetic deletions in muscle cells and adeno-associated virus–mediated overexpression of FGF-2 or SPARC in mouse skeletal muscle revealed that this axis regulates differentiation of fibro/adipogenic progenitors in vitro and intramuscular adipose tissue (IMAT) formation in vivo. Skeletal muscle from human donors aged >75 y versus <55 y showed activation of FGF-2–dependent signaling and increased IMAT. Thus, our data highlights a disparate role of FGF-2 in adult skeletal muscle and reveals a pathway to combat fat accumulation in aged human skeletal muscle.**

skeletal muscle | FGF-2 | SPARC | FRA-1 | IMAT

Skeletal muscle is a fundamental organ for the health of the human body (1). It comprises 40% of whole-body mass and ensures movement, posture, and stability. Moreover, skeletal muscle participates in heat production and whole-body metabolism. Decreased glucose uptake in muscle tissue promotes de novo lipogenesis in the liver (2) while the capacity of skeletal muscle to oxidize fatty acids determines weight gain and obesity (3). The activation of skeletal muscle during exercise can have beneficial effects on sympathetic activity and inflammation (4) as well as on the secretion of myokines into the blood stream (5). Strategies to maintain muscle mass and function are therefore pivotal to prevent morbidity in the population.

Aging, obesity, and muscle disuse pose a major threat to muscle health in the society. Starting at 40 y of age, muscle mass declines by 8% per decade (6). Although this process is variable, in older adults, the loss of muscle mass can decline more than 2 SDs below the mean of young healthy adults. This drastic decrease in muscle mass is defined as sarcopenia and is a key contributor to adverse events in the elderly such as falls, disability, and death, which are summarized under the term frailty (7). Once muscle mass decreases, a decline of the basal metabolic rate follows. The consequence is an increasing prevalence of obesity, skeletal muscle insulin resistance, and type 2 diabetes mellitus in the group of people aged 65 or older (8, 9).

The molecular mechanisms that contribute to the decrease in skeletal muscle mass during aging and type 2 diabetes are complex and still incompletely understood. However, a unique feature of muscle during aging, obesity, and type 2 diabetes is the appearance of adipose tissue between skeletal muscle fibers, the intramuscular adipose tissue (IMAT) (10–12). In overweight subjects (body mass index between 28 and 30 kg/m$^2$), the amount of IMAT can be substantial and is estimated to relate to 5% (women) or 10% (men) of whole-body adipose tissue (11). IMAT is generally associated with systemic insulin resistance (11, 13), decreased muscle strength (14), and, in older adults, impaired mobility (15–17). A large body of work over the last years have addressed the origin of IMAT. Skeletal muscle contains preadipocyte progenitors termed fibro/adipogenic progenitors (FAPs) that normally do not form adipocytes but proliferate during muscle injury to support the commitment of myogenic progenitor cells (MPs) during muscle repair (18). However, under the conditions outlined above, rather than undergoing apoptosis, FAPs differentiate to adipocytes and give rise to IMAT (18–20). The molecular cues that trigger this pathogenesis are unknown and warrant further investigation.

Here, we expose the fickle role of FGF-2, which participates not only in the growth of myogenic progenitors and fibers but also supports the differentiation of FAPs. By following upstream and downstream signaling events of a master regulator of myogenesis, microRNA (miR)-29a (21), we identified an intricate FGF-2 signaling pathway in muscle cells, which enhances differentiation of FAPs in vitro and promotes IMAT formation in vivo during muscle regeneration via the suppression of the myokine SPARC. Additionally, the FGF-2/miR-29a/SPARC pathway is enhanced in

## Significance

A unique feature of muscle during aging, obesity, and type 2 diabetes is the appearance of adipose tissue between skeletal muscle fibers, the intramuscular adipose tissue (IMAT). IMAT is generally associated with insulin resistance, decreased muscle strength, and, in older adults, impaired mobility. However, the molecular cues that cause the pathological formation of IMAT are currently unknown. This work uncovers a conserved FGF-2–mediated signaling axis that up-regulates the expression of microRNA-29a, triggering a decrease of the adipogenic inhibitor SPARC and increased fat formation in aged skeletal muscle. We show that FGF-2–dependent signaling modulates the fate of fibro/adipogenic progenitors and their propensity to differentiate to intramuscular adipocytes, which reveal therapeutic opportunities to prevent IMAT formation in human skeletal muscle.

Author contributions: S.M. and J.K. designed research; S.M. and A.F. performed research; C.W. contributed new reagents/analytic tools; S.M., A.F., U.G., and J.K. analyzed data; S.M. and J.K. wrote the paper; and H.A.R. and M.L. recruited patients and performed muscle biopsies.

The authors declare no competing interest.

This article is a PNAS Direct Submission.



[1]To whom correspondence may be addressed. Email: Jan.Kruetzfeldt@usz.ch.

This article contains supporting information online at https://www.pnas.org/lookup/suppl/doi:10.1073/pnas.2021013118/-/DCSupplemental.

Published September 7, 2021.

aged skeletal muscle of mice and humans. Our findings reveal an unexpected side of FGF-2 action that could provide new strategies to prevent IMAT formation in the aged skeletal muscle.

## Results

**SPARC Is a Conserved Target of miR-29a in Skeletal Muscle.** We have previously shown that miR-29a is a master regulator of muscle cell differentiation in vitro (21) and muscle regeneration in vivo (22). Interestingly, the inhibition of miR-29a in the muscle cell line C2C12 affected adipogenic differentiation of 3T3 cells in a coculture system (Fig. 1*A*). To understand how the inhibition of miR-29a in muscle cells decreases adipogenic differentiation, we embarked on identifying secreted targets of miR-29a that participate in crosstalk between skeletal muscle and adipocytes. We used both trancriptomics and proteomics datasets in which miR-29a was down-regulated in human primary myoblasts and C2C12 myotubes, respectively. We have previously published an RNA deep sequencing dataset of human myotubes (21), which we now reanalyzed specifically for miR-29a targets. For the proteomics dataset, liquid chromatography–mass spectrometry (LC-MS/MS) was performed on the supernatants of C2C12 myotubes. Successful silencing of miR-29a was confirmed using a right shift in the cumulative distribution fractions plots of the predicted miR-29a target genes compared to nontargets (*SI Appendix*, Fig. S1 *A* and *B*) as well as by using enrichment plot analysis (*SI Appendix*, Fig. S1 *C* and *D*) in both experimental conditions. The silencing of miR-29a during the differentiation of human myoblasts significantly up-regulated 3,827 genes and down-regulated 3,497 genes

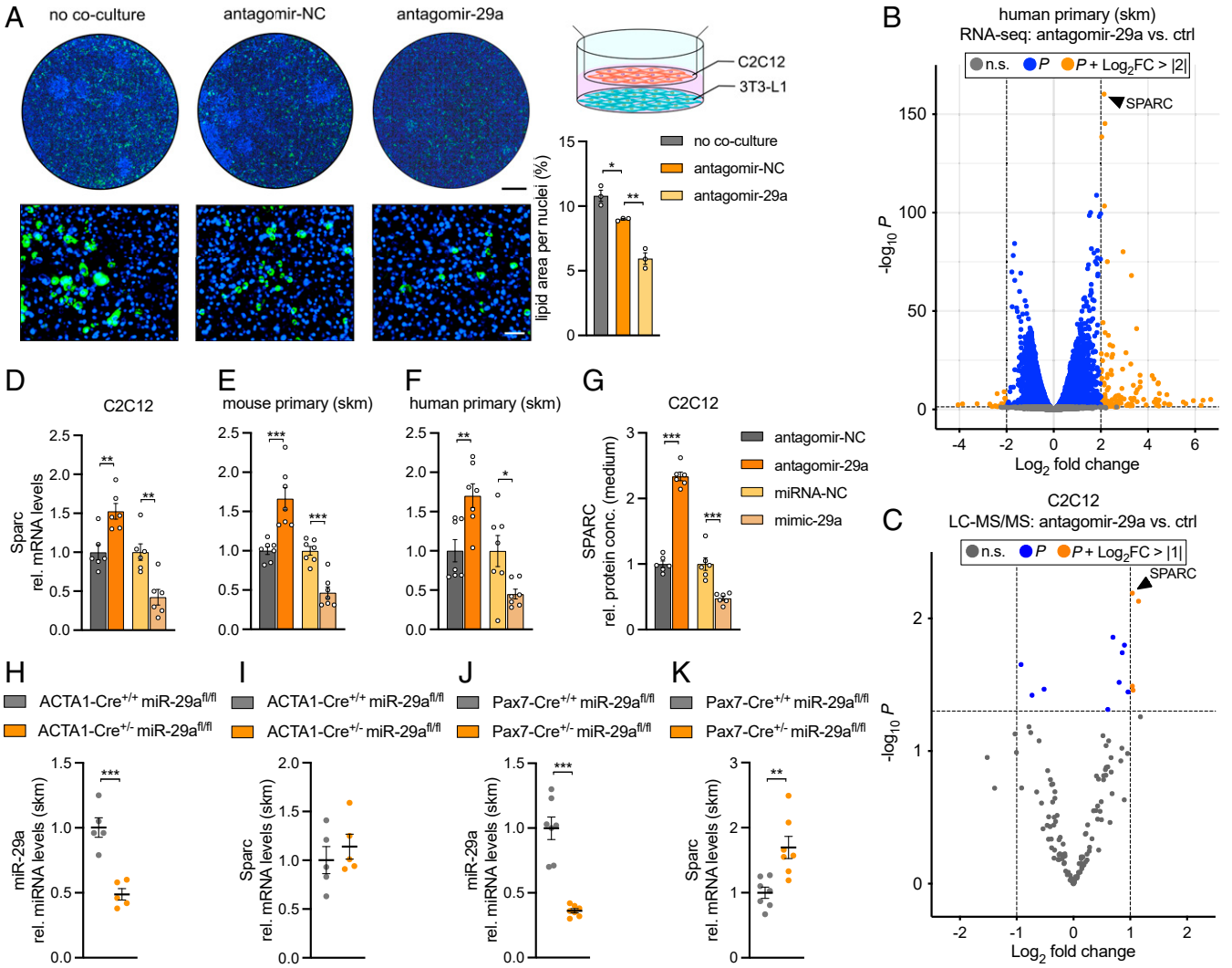


**Fig. 1.** SPARC is regulated by miR-29a in skeletal muscle both in vitro and in vivo. (*A*) Coculture of C2C12 myotubes, transfected with antagomir negative control (NC) or antagomir-29a and 3T3-L1 cells. No coculture control shows 3T3-L1 cells cultured without C2C12 myotubes. Representative images show lipid droplet (Bodipy; green) and nuclei (Hoechst; blue) staining of 3T3-L1 cells on day 8 after induction of adipogenesis. Lipid area was normalized to nuclei ($n = 3$). (Scale bar, 5 mm, *Top*; 100 μm, *Bottom*.) (*B* and *C*) Volcano plots (significance versus $\log_2$ FC) of significantly altered (*B*) genes ($n = 3$; FC > |2| and $P < 0.05$) or (*C*) proteins ($n = 4$; FC > |1| and $P < 0.05$) after inhibition of miR-29a; n.s. = not significant. (*D–F*) Sparc expression in (*D*) C2C12 myotubes ($n = 6$), (*E*) mouse primary myotubes ($n = 7$), and (*F*) human primary myotubes ($n = 7$) after inhibition or overexpression of miR-29a. qPCR values were normalized to 18S ribosomal RNA (rRNA) and plotted relative to negative control antagomir or mimic. (*G*) Levels of secreted SPARC in conditioned medium from C2C12 myotubes after inhibition or overexpression of miR-29a as assessed by enzyme-linked immunosorbent assay ($n = 6$). SPARC levels are plotted relative to negative control antagomir or mimic. (*H* and *J*) miR-29a and (*I* and *K*) Sparc expression in ACTA1-Cre miR-29a$^{fl/fl}$ versus miR-29a$^{fl/fl}$ ($n = 5$) or Pax7-Cre miR-29a$^{fl/fl}$ versus miR-29a$^{fl/fl}$ mice ($n = 7$). qPCR values were normalized to 18S rRNA (Sparc) or snoRNA234 (miR-29a). Data in *A* and *D–K* are plotted as mean ± SEM. Significance was evaluated by (*A*) one-way ANOVA with Tukey's multiple comparisons test, (*B* and *C*) differential expression statistic (Benjamini–Hochberg adjusted *P* value), and (*D–K*) two-tailed unpaired Student's *t* test. *$P \leq 0.05$ **$P \leq 0.01$; ***$P \leq 0.001$.

with a $P$ value < 0.05, while the silencing of miR-29a in myotubes significantly increased the abundance of 79 proteins and decreased 54 proteins ($P < 0.05$) in the supernatant. To enrich for secreted proteins with potential functions in crosstalk, LC-MS/MS data were filtered for direct targets of miR-29a-3p using TargetScan v7.2, while proteins providing structural support were excluded (10 proteins, annotated as Extracellular Matrix Component; Gene Ontology term 0044420). The secreted myokine (23) and miR-29a target (24) Secreted protein acidic and rich in cysteine (SPARC) was the most significantly up-regulated gene and protein in both the transcriptomic and proteomic datasets (Fig. 1 *B* and *C*). *SI Appendix*, Table S1 provides a full list of the significantly changed proteins and their potential role in adipogenesis. We used three strategies to provide evidence that SPARC is a direct target of miR29a in skeletal muscle. First, in vitro, enhanced, or repressed SPARC levels in response to treatments with miR-29a antagomirs or mimics was detected at the messenger RNA (mRNA) level and as secreted protein in C2C12 myotube cultures (Fig. 1 *D* and *G*) as well as at the mRNA level and as secreted protein in primary mouse and primary human myotubes (Fig. 1 *E* and *F* and *SI*

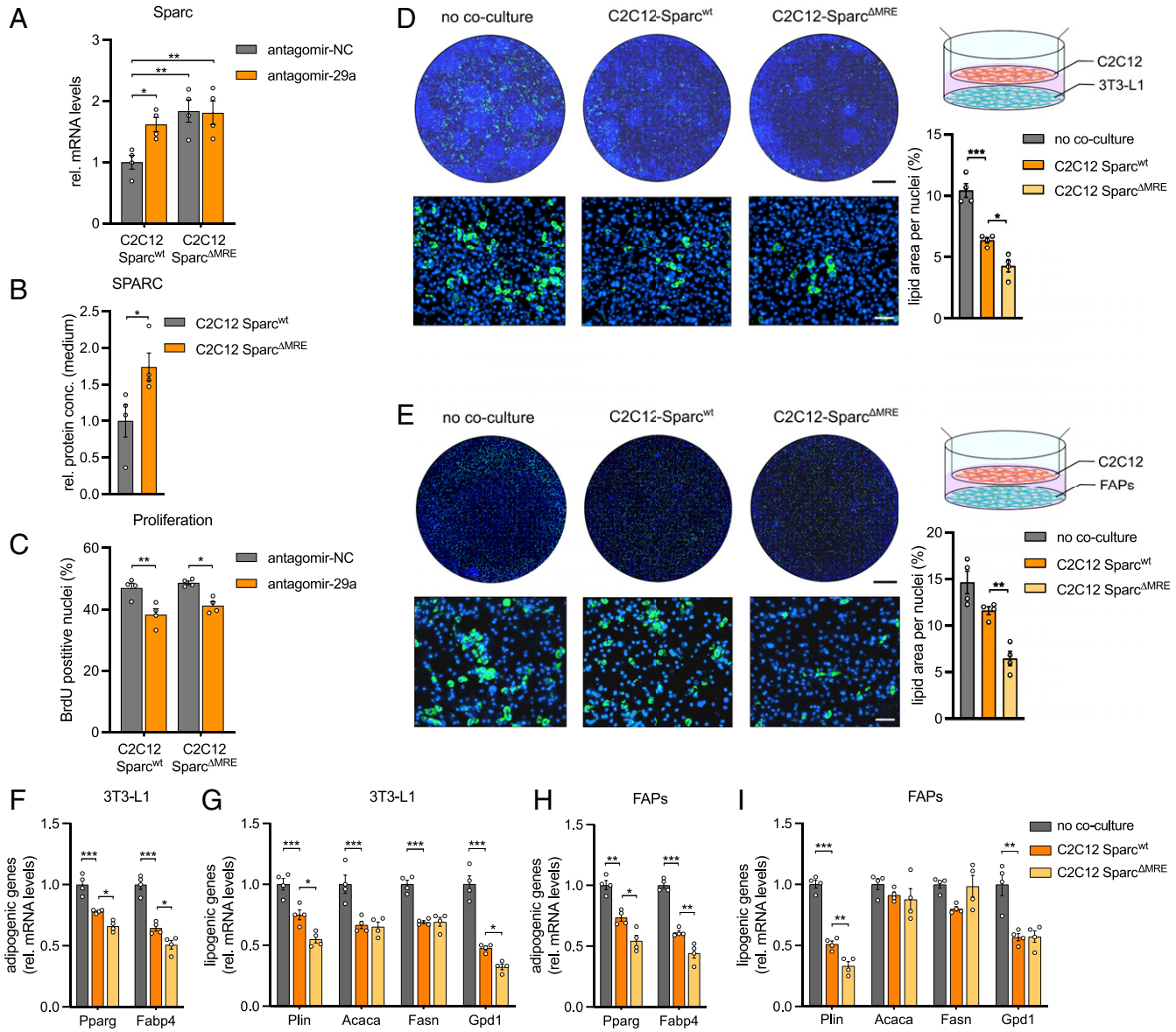


**Fig. 2.** miR-29a promotes adipogenesis via down-regulation of SPARC in vitro. (*A*) Sparc expression in wild-type (wt) or C2C12 myoblasts with deleted miR-29a recognition elements (C2C12 Sparc$^{\Delta MRE}$) after inhibition of miR-29a ($n = 4$). qPCR values were normalized to 18S ribosomal RNA (rRNA). (*B*) Levels of secreted SPARC in conditioned medium from wt or C2C12 myoblasts with deleted miR-29a recognition elements (C2C12 Sparc$^{\Delta MRE}$) as assessed by enzyme-linked immunosorbent assay ($n = 4$). (*C*) Cell proliferation in wt or C2C12 cells with deleted miR-29a recognition elements (C2C12 Sparc$^{\Delta MRE}$) after inhibition of miR-29a ($n = 4$). (*D* and *E*) Coculture of wt or C2C12 myotubes with deleted miR-29a recognition elements (C2C12 Sparc$^{\Delta MRE}$) and (*D*) 3T3-L1 ($n = 4$) or (*E*) FAPs ($n = 4$). No coculture control shows 3T3-L1 cells or FAPs cultured without C2C12 myotubes. Representative images show lipid droplet (Bodipy; green) and nuclei (Hoechst; blue) staining of 3T3-L1 or FAPs on day 8 after induction of adipogenesis. Lipid area was normalized to nuclei. (Scale bar, 5 mm, *Top*; 100 μm, *Bottom*.) (*F–I*) Adipogenic and lipogenic gene expression of (*F* and *G*) 3T3-L1 cells or (*H* and *I*) FAPs cocultured with C2C12 Sparc$^{wt}$ or C2C12 Sparc$^{\Delta MRE}$ myotubes on day 8 after induction of adipogenesis ($n = 4$). No coculture control shows 3T3-L1 cells or FAPs cultured without C2C12 myotubes. qPCR values were normalized to 18S rRNA. All data are plotted as mean ± SEM. Significance was evaluated by (*A* and *C–I*) one-way ANOVA with Tukey's multiple comparisons test and (*B*) two-tailed unpaired Student's *t* test. *$P \le 0.05$; **$P \le 0.01$; ***$P \le 0.001$.

*Appendix*, Fig. S1 *E* and *F*). Second, in vivo, we used two knockout models of miR-29a in the adult skeletal muscle of mice: ACTA1-Cre-miR-29a$^{fl/fl}$, which achieved 50% depletion of the miRNA (Fig. 1*H*), and Pax7-Cre-miR-29a$^{fl/fl}$, in which miR-29a was depleted by 70% (Fig. 1*J*). Only miR-29a depletion by 70% resulted in increased Sparc expression in adult skeletal muscle, indicating a miRNA target gene threshold requiring >50% knockdown of miR-29a (Fig. 1 *I* and *K*). Third, to prove that SPARC is indeed a direct target of miR-29a, we deleted two predicted and conserved binding sites for miR-29a in the 3′ untranslated region (UTR) of SPARC. The deletion of these sites relieved the miR-29a–dependent repression in reporter gene assays (*SI Appendix*, Fig. S1 *G* and *H*). Together, our results identify Sparc as a conserved regulated target of miR-29a in skeletal muscle both in vitro and in vivo. Therefore, we hypothesized that the inhibition of miR-29a in muscle cells leads to the up-regulation and subsequent secretion of SPARC, resulting in the suppression of adipogenic differentiation in the coculture system.

**The miR-29a/SPARC Axis Regulates Skeletal Muscle Preadipocyte Differentiation In Vitro.** To assess the functional role of SPARC downstream of miR-29a as a potential modulator of FAP cell fate, we generated four C2C12 cell lines with genomic deletions of the miR-29a recognition elements (MRE) in the Sparc 3′ UTR using CRISPR/Cas9 (Sparc$^{\Delta MRE}$, *SI Appendix*, Fig. S2*A*). The up-regulation of Sparc at the protein level, where its abundance in the supernatant of the mutant versus wild-type cells was elevated by approximately twofold, was mirrored by an almost twofold up-regulation at the mRNA level, in both myoblasts and myotubes (Fig. 2 *A* and *B*, and *SI Appendix*, Fig. S2*B*). Strikingly, the inhibition of miR-29a in the mutant cells did not cause a further increase in SPARC mRNA, proving definitely that SPARC regulation after miR-29a inhibition is caused directly by miR-29a binding. The proliferation capacity of C2C12 myoblasts after miR-29a inhibition was decreased (Fig. 2*C*), a hallmark of miR-29a action in muscle cells (22). This phenotype was also present in the C2C12 Sparc$^{\Delta MRE}$ cells, indicating that Sparc does not participate in intrinsic signaling events in muscle cells downstream of miR-29a (Fig. 2*C*). To assess if SPARC influences the differentiation capacity of adipocyte progenitors, we cocultured Sparc$^{wt}$ or Sparc$^{\Delta MRE}$ cell lines with 3T3 cells or FAPs isolated from murine skeletal muscle (Fig. 2 *D–I*). Sparc$^{\Delta MRE}$ cells strongly inhibited the differentiation of both 3T3 preadipocytes as well as FAPs and reduced adipogenic and lipogenic gene expression in both cell types as compared to Sparc$^{wt}$ cells. The inhibition of FAPs differentiation could be a direct effect of SPARC, at least in part, as the incubation of FAPs with recombinant SPARC was also able to reduce the differentiation of FAPs (*SI Appendix*, Fig. S2 *C–E*). Importantly, SPARC elevation did not change the fibrogenic, osteogenic, or smooth muscle programs in FAPs (*SI Appendix*, Fig. S2 *F–H*). Reducing Sparc levels in C2C12 cells during the coculture experiments using endoribonuclease-prepared small interfering RNA (esiRNA) increased adipocyte differentiation at baseline and in the presence of antagomir-29a (*SI Appendix*, Fig. S2*I*). Moreover, reducing Sparc levels prevented the inhibitory effect of antagomir-29a on adipocyte differentiation. Importantly, the effect of antagomir-29a on 3T3 cell differentiation and esiRNA against Sparc on FAPs differentiation is not limited to C2C12 cells but can also be observed in primary muscle cells from mice and humans (*SI Appendix*, Fig. S2 *J–S*). Together, these results indicate that the miR-29a/SPARC axis is a regulator of adipocyte differentiation that mediates the crosstalks between muscle cells and preadipocytes residing in adult skeletal muscle.

**An FGF-2/MEK1/2/MAPK Signaling Axis Regulates Sparc via miR-29a.** Since miR-29a regulates FAP cell fate, we decided to decipher the regulatory pathway upstream of this pivotal miRNA. Among several growth factors and hormonally relevant cues for skeletal muscle, only FGF-2 was able to induce miR-29a in C2C12 myotubes (Fig. 3*A*), in line with our previous published observations that miR-29a/b1 is the highest regulated miRNA cluster by FGF-2 in primary human myoblasts (22). A total of 24 h posttreatment, FGF-2 induced a dose-dependent up-regulation of miR-29a (*SI Appendix*, Fig. S3 *A* and *B*) and a reciprocal down-regulation of SPARC transcript (Fig. 3*B*). Strikingly, FGF-2–mediated inhibition of Sparc was abolished in the C2C12 Sparc$^{\Delta MRE}$ cell lines, implicating that FGF-2, miR-29a, and SPARC belong to the same signaling pathway (Fig. 3*C*). To identify signaling events downstream of FGF-2 that mediate miR-29a expression, we cloned 1,867 base pairs (bp) of the published miR-29a promoter (25) into a luciferase reporter vector. Promoter activation by FGF-2 was localized to a 590-bp fragment (Fig. 3*D* and *SI Appendix*, Fig. S3*C*), which was used in subsequent experiments with chemical inhibitors to numerous intracellular pathways downstream of FGF-2 (26). Overall, we silenced the FGF-2 receptor (PD173074), RAS-MAPK signaling (PD184352, targeting MEK1/2; NSC23766, targeting Rac GTPase), PI3K-AKT signaling (LY294002, targeting PI3Kα/δ/β), PLC-γ signaling (U73122), and STAT signaling (Nifuroxazide) in the presence of FGF-2. Notably, the suppression of FGF-2–activated miR-29a promoter activity was mostly dependent on the inhibition of MAPK/ERK kinase 1/2 (MEK1/2) (Fig. 3*E*), which was mimicked by the overexpression of a dominant active form of MEK2 (Fig. 3*F*). While the PD inhibitor significantly reduced the promoter activity also in the absence of FGF-2, U73122 had no effect alone (*SI Appendix*, Fig. S3*D*). In primary myotubes, FGF-2 treatment increased the phosphorylation of p44/42 MAPK, the downstream target of MEK1/2 (Fig. 3*G*). Additionally, in both myoblasts and myotubes from both mice and humans, MEK1/2 inhibition also prevented the FGF-2–mediated induction of miR-29a (Fig. 3 *H–J* and *SI Appendix*, Fig. S3 *E* and *F*) and increased expression of the miR-29a target Sparc (Fig. 3 *K–M* and *SI Appendix*, Fig. S3 *G* and *H*). Interestingly, MEK1/2 inhibition also affected miR-29a levels and Sparc expression in the absence of FGF-2. However, the effect size was much smaller as compared to the regulation in the presence of FGF-2 and might indicate endogenous activation of the FGF-2 signaling pathway in muscle cells. Together, these results establish that MEK1/2 acts upon the miR-29a promoter and relegates Sparc to a pathway involving FGF-2 signaling via MEK1/2, p44/42 MAPK, and miR-29a.

**The Transcription Factor FRA-1 is Up-Regulated by FGF-2 to Induce miR-29a Expression.** To identify all participants in the signal transduction cascade that determines the expression of miR-29a and Sparc, we pursued the identity of the transcription factor (TF) that mediates the effect of FGF-2/MEK1/2 on the miR-29a promoter. We further narrowed down the promoter region (Fig. 4*A*) and identified a 97-bp promoter fragment (−374 to −278 bp upstream of the transcription start site) that preserved its dependence on MEK1/2 inhibition and MEK2 stimulation (Fig. 4 *B* and *C*). Since the fragment −374 to −312 did not show promoter activity, we focused on a 54-nucleotide (nt) promoter region located at −331 to −278 bp. Bioinformatic analysis revealed 55 potential *cis*-regulatory elements in this region with 12 TF-binding sites showing a relative match score >0.9. We performed site-directed mutagenesis to sequentially abolish TF binding on the 54-nt promoter region within the 97-bp fragment and identified a conserved Fos–Jun consensus site, which is bound by members of the activating protein-1 (AP-1) family of TFs and responsive to FGF-2 stimulation (Fig. 4 *D* and *E*). The mutation of this site successfully prevented MEK2-stimulated increase of promoter activity compared to the wild-type promoter fragment (Fig. 4*F*). DNA-binding activity of the AP-1 family is modulated via phosphorylation and through its homo- or heterodimer composition, which is determined by differential expression of the AP-1 protein members Jun, Fos, activating TF (ATF), and musculoaponeurotic fibrosarcoma

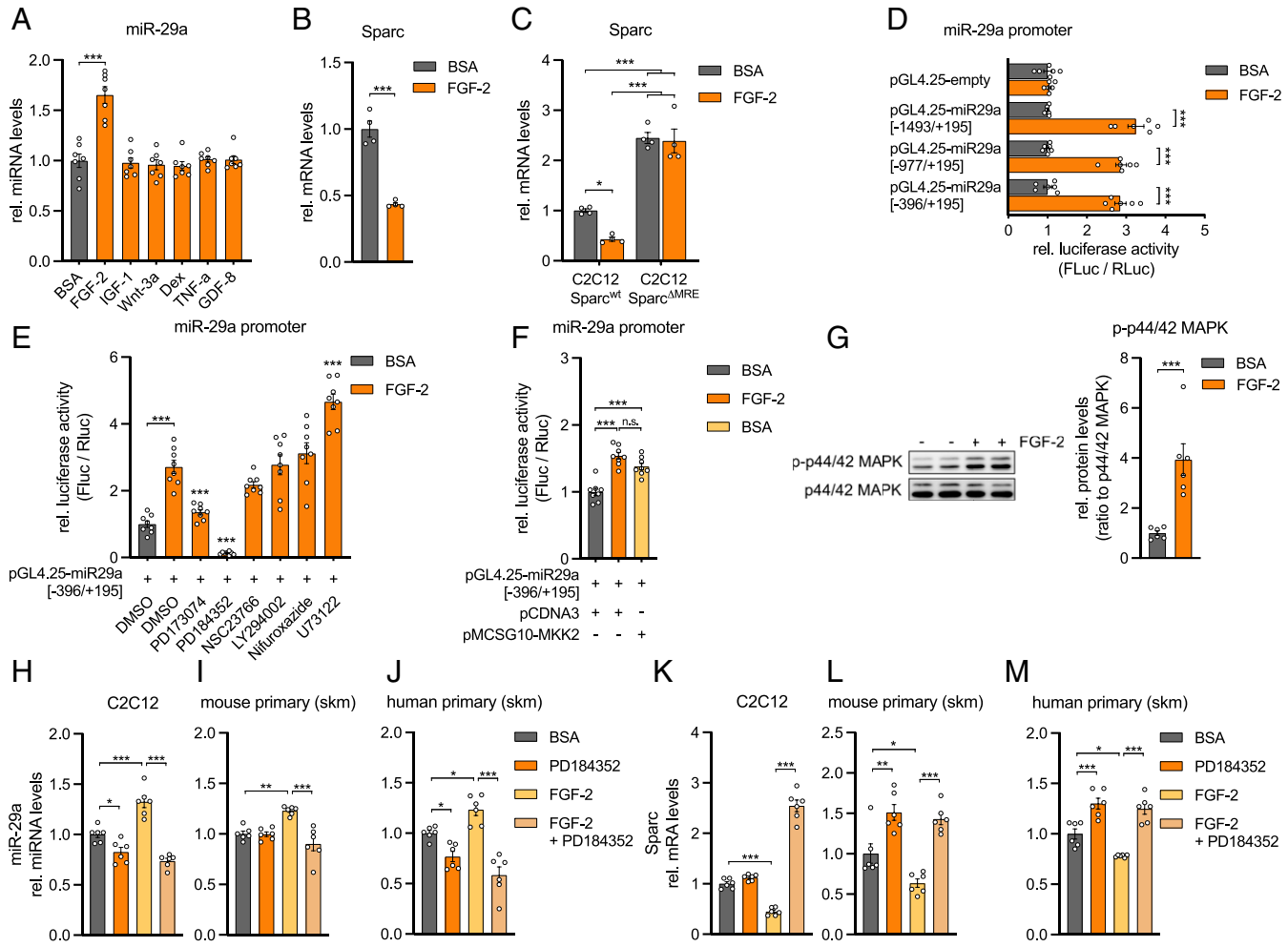


**Fig. 3.** FGF-2 signaling decreases Sparc via MEK1/2, p42/44 MAPK, and miR-29a. (*A*) miR-29a expression in C2C12 myotubes after treatment with respective recombinant proteins or dexamethasone ($n = 7$). qPCR values were normalized to snoRNA234. (*B* and *C*) Sparc expression in (*B*) C2C12 myotubes ($n = 4$) or in (*C*) wild-type and C2C12 myoblasts with deleted miR-29a recognition elements (C2C12 Sparc$^{\Delta MRE}$; $n = 4$) after treatment with recombinant FGF-2. qPCR values were normalized to 18S ribosomal RNA (rRNA). (*D*) miR-29a promoter activity for full-length (−1,493/+195) and truncated (−977/+195, −396/+195) promoter constructs after treatment with recombinant FGF-2 ($n = 6$). (*E*) miR-29a promoter activity for truncated (−396/+195) promoter construct after treatment with inhibitors against FGFR1 (PD173074), MEK1/2 (PD184352), Rac GTPase (NSC23766), PI3Kα/δ/β (LY294002), STAT1/3/5 (Nifuroxazide), PLC (U73122), and recombinant FGF-2. Stars indicate significant difference compared to dimethyl sulfoxide control treated with FGF-2 ($n = 8$). (*F*) miR-29a promoter activity for truncated (−396/+195) promoter construct after treatment with recombinant FGF-2 or overexpression of MEK2 (MKK2) ($n = 8$). Experiments in *D*–*F* were performed in C2C12 myotubes and assessed by normalized luciferase assays. (*G*) Immunoblot depicting phosphorylation of p44/42 MAPK in C2C12 myotubes treated with recombinant FGF-2 ($n = 6$). Band densities were quantified and normalized to total p44/42 MAPK. (*H*–*J*) miR-29a and (*K*–*M*) Sparc expression in (*H* and *K*) C2C12 myotubes, (*I* and *L*) mouse primary myotubes, and (*J* and *M*) human primary myotubes after treatment with recombinant FGF-2 and inhibition of MEK1/2 signaling (PD184352; $n = 6$). qPCR values were normalized to snoRNA234 (miR-29a) or 18S rRNA (Sparc). All data are plotted as mean ± SEM. Significance was evaluated by (*A*, *C*–*F*, and *H*–*M*) one-way ANOVA with (*A* and *E*) Dunnett's or (*C*, *D*, *F*, and *H*–*M*) Tukey's multiple comparisons test and (*B* and *G*) two-tailed unpaired Student's *t* test. n.s. = not significant; $*P \leq 0.05$; $**P \leq 0.01$; $***P \leq 0.001$.

(MAF) (27). Among the Fos/Jun family members, Fos-related antigen 1 (Fosl1, encodes protein FRA-1) gene expression was strongly induced by FGF-2 and markedly down-regulated by MEK1/2 inhibition (Fig. 4*G*). Overexpression of the Fosl1 gene in C2C12 cells and primary mouse myoblasts activated the miR-29a promoter in the absence of FGF-2 (Fig. 4 *H*–*J*), and the knockdown of Fosl1 prevented the FGF-2–stimulated increase in miR-29a promoter activity (Fig. 4*K*). Adeno-associated virus (AAV)-mediated overexpression of Fosl1 induced miR-29a expression (Fig. 4 *L* and *M*), and the knockdown of Fosl1 prevented the induction of miR-29a expression by FGF-2 (Fig. 4*O*). Finally, in cultured human myoblasts, FGF-2 treatment significantly increased phosphorylation of FRA-1 (*SI Appendix*, Fig. S4). Chromatin immunoprecipitation (ChIP) analysis successfully demonstrated that phosphorylated FRA-1 occupies the promoter of miR-29a in human myoblasts. This relationship is significantly increased by fivefold in the presence of FGF-2 (Fig. 4*P*). Together, our results define an FGF-2/FRA-1/miR-29a/SPARC axis that is conserved in skeletal muscle cells from mice and humans.

**Aged Mice Have Higher Levels of the TF p-FRA-1.** Next, we wanted to understand whether the FGF-2 signaling pathway that we identified in vitro is also active in skeletal muscle in vivo. Since FGF-2 abundance is increased in skeletal muscle during aging in mice (28, 29), we turned to 25-mo-old aged mice and compared them to two-mo-old mice (young control). Indeed, aged mice had a higher expression of Fgf2, Fosl1, and miR-29a (Fig. 5 *A*–*C*). Importantly, Sparc expression and circulating SPARC levels were also lower in the aged mice (Fig. 5 *D* and *E*). Moreover, we successfully demonstrated that aged skeletal muscle is characterized by higher

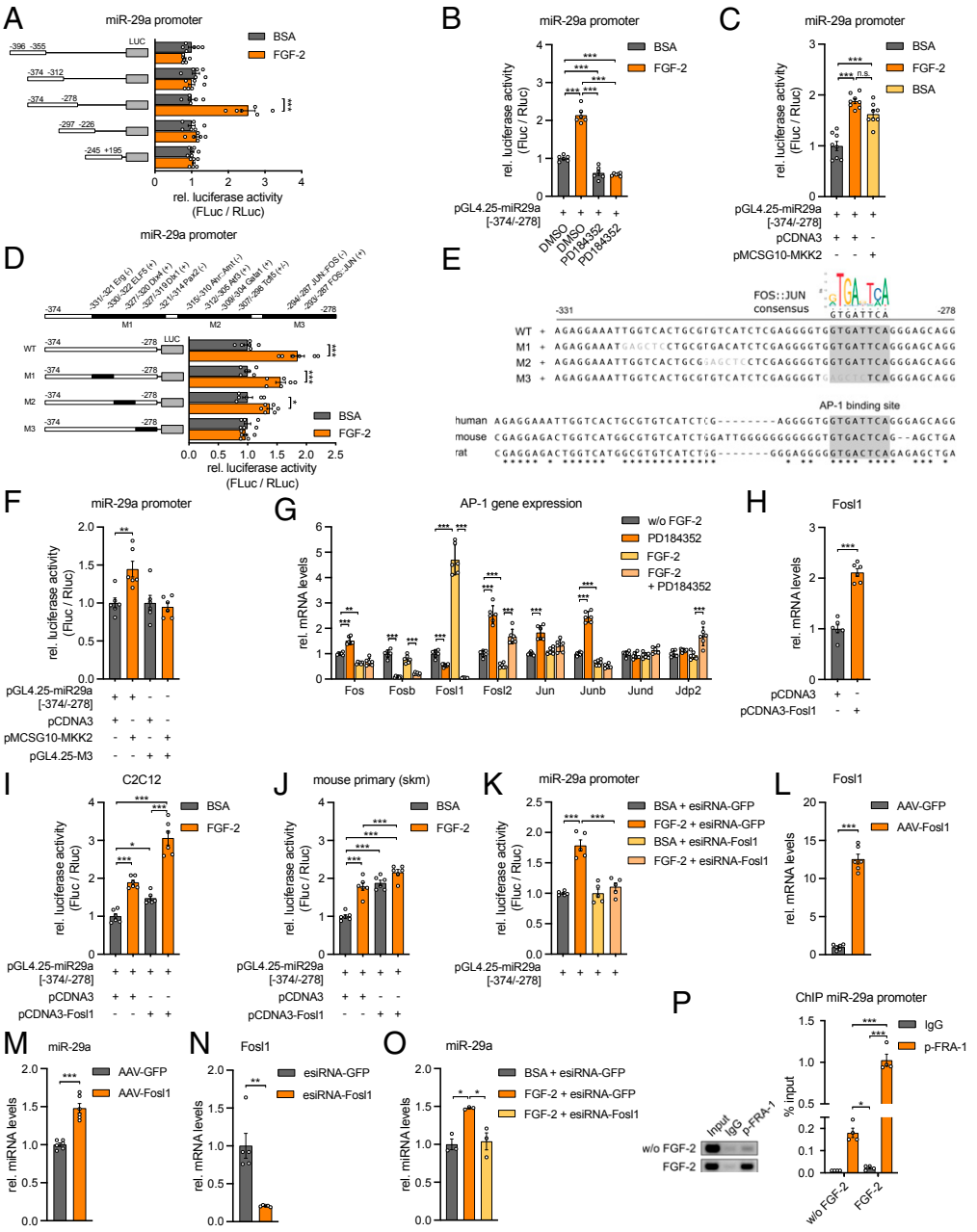


**Fig. 4.** The TF FRA-1 mediates miR-29a expression downstream of FGF-2. (*A*) miR-29a promoter activity for truncated promoter constructs as indicated and treatment with recombinant FGF-2 ($n$ = 6). (*B* and *C*) miR-29a promoter activity for truncated promoter construct (−374/−278) after treatment with recombinant FGF-2 and (*B*) inhibition ($n$ = 6) or (*C*) activation ($n$ = 8) of MEK1/2 signaling (MKK2). (*D*) miR-29a promoter activity for truncated wild type (wt) or mutated (M1, M2, M3) promoter constructs after treatment with recombinant FGF-2 ($n$ = 6). Respective mutageneses abolished binding of indicated transcription factors located either on a sense (+) or antisense (−) strand. *Cis*-regulatory elements are given in relation to transcription start site. (*E*) Depicted are wt and mutated (M1, M2, M3) miR-29a promoter sequences used in *D* and *F*. Mutated nucleotides are shown in gray letters. Motif analysis revealed a conserved Fos–Jun-binding site removed in mutant 3 (M3). Stars indicate identical nucleotides among species. (*F*) miR-29a promoter activity for truncated wt (−374/−278) or mutated (M3) promoter constructs after activation of MEK2 signaling (MKK2; $n$ = 6). (*G*) Gene expression of indicated AP-1 transcription factors in C2C12 myotubes after treatment with recombinant FGF-2 and inhibition of MEK1/2 signaling ($n$ = 6). (*H*) Fosl1 expression in C2C12 myoblasts after overexpression of Fosl1 ($n$ = 6). (*I* and *J*) miR-29a promoter activity for truncated promoter construct (−374/278) after treatment with recombinant FGF-2 and/or overexpression of Fosl1, performed in (*I*) C2C12 myoblasts or (*J*) mouse primary myoblasts ($n$ = 6). (*K*) miR-29a promoter activity for truncated promoter construct (−374/−278) after treatment with recombinant FGF-2 and/or knockdown of Fosl1 ($n$ = 5). (*L* and *M*) *L* Fosl1 and *M* miR-29a expression in mouse primary myotubes after AAV-mediated overexpression of Fosl1 ($n$ = 6). (*N*) Fosl1 expression in mouse primary myoblasts after knockdown of Fosl1 ($n$ = 5). (*O*) miR-29a expression in mouse primary myoblasts after treatment with recombinant FGF-2 and knockdown of Fosl1 ($n$ = 3). (*P*) ChIP of p-FRA1 on miR-29a promoter performed in human primary myoblasts after treatment with recombinant FGF-2 ($n$ = 4). miR-29a promoter enrichment was assessed relative to total input DNA by qPCR and is depicted in relation to negative control (IgG). Representative samples were visualized on an agarose gel (*Left*). Data in *A*–*D*, *F*, and *K* were performed in C2C12 myotubes and assessed by normalized luciferase assays. qPCR values in *G*, *H*, and *L*–*O* were normalized to snoRNA234 (miR-29a) or 18S rRNA. All data are plotted as mean ± SEM. Significance was evaluated by (*A*–*D*, *F*, *I*–*K*, *O*, and *P*) one-way ANOVA with Tukey's multiple comparisons test, (*G*) two-way ANOVA with Tukey's multiple comparisons test, and (*H* and *L*–*N*) two-tailed unpaired Student's *t* test. n.s. = not significant; $*P \leq 0.05$; $**P \leq 0.01$; $***P \leq 0.001$.

levels of phosphorylated FRA-1 and that FRA-1 binding to the miR-29a promoter is significantly increased in aged versus young mice as revealed by ChIP analysis (Fig. 5 *F* and *G*). Importantly, FAPs isolated from aged mice retained a similar sensitivity to SPARC-induced inhibition of adipogenesis as compared to FAPs isolated from young mice (*SI Appendix*, Fig. S5), indicating that the decreased Sparc levels that we observed in skeletal muscle from aged mice could be relevant for the FAPs. We conclude that the FGF-2/FRA-1/miR-29a/SPARC axis is consistently regulated in vivo in aged skeletal muscle of mice and could affect aging-related IMAT.

**FGF-2 and SPARC Regulate IMAT Formation.** To demonstrate the function of the FGF-2 /SPARC axis as a regulator of adipocyte differentiation in vivo, we employed the glycerol model of muscle regeneration in which fatty infiltration can be readily observed (20) as opposed to other mouse models such as denervation atrophy (30–33) or cancer cachexia (34–37). To this end, we injected Fgf2 or Sparc-overexpressing AAV 9 directly into the tibialis anterior muscle of mice as previously described (38–42). This approach is expected to infect both type 1 and type 2 fibers but not adult muscle stem cells (42). After 3 wk, muscle regeneration and fatty infiltration was induced using a single glycerol injection, and 2 wk later, muscles were analyzed for adipocyte infiltration (Fig. 6*A*). AAV-Fgf2 induced Fgf2 expression and increased muscle mass (Fig. 6 *B* and *C*). Importantly, IMAT formation was drastically induced in paraffin sections from AAV-Fgf2 compared to AAV-GFP–injected muscle where IMAT area and total adipocyte number were significantly increased by 12-fold and ninefold, respectively (Fig. 6*F*). Accordingly, at the molecular level, fatty acid–binding protein 4 (Fabp4) and peroxisome proliferator–activated receptor gamma (Pparg) were significantly up-regulated (Fig. 6 *D* and *E*). Strikingly, overexpression of Sparc using the same AAV approach (Fig. 6*G*) led to the opposite effect. IMAT formation and total adipocyte number were significantly decreased by more than 50% with the AAV-Sparc versus AAV-GFP virus (Fig. 6*J*). This decrease in adipocyte infiltration was accompanied by a significant decrease in the expression of adipocyte markers Fabp4 and Pparg (Fig. 6 *H* and *I*). Interestingly, FAPs numbers changed in the same direction as IMAT after the introduction of both AAV-Fgf2 or AAV-Sparc (*SI Appendix*, Fig. S6 *A–F*), but these effects were more subtle and unlikely explain the pronounced effects that we observed for IMAT formation. We conclude that the FGF-2/SPARC axis regulates the differentiation of FAPs in vitro and IMAT formation in vivo (see Fig. 7). Importantly, AAV-Sparc also reduced IMAT in aged mice (*SI Appendix*, Fig. S6 *G–J*), providing further support for the role of FGF-2/SPARC in aging-related IMAT.

**FGF-2–Dependent Signaling Is Activated in Aged Human Skeletal Muscle.** Lastly, we asked whether the FGF-2–dependent signaling pathway that regulates SPARC is also activated in aged skeletal muscle from humans (patient characteristics in *SI Appendix*). Similarly to aged skeletal muscle from mice, in aged human muscle, the expression of miR-29a was significantly up-regulated, while its target gene SPARC was significantly down-regulated as compared to young human muscle (Fig. 8 *C* and *D*). While the up-regulation of FGF2 and FOSL1 did not reach statistical significance (Fig. 8 *A* and *B*), FGF-2 expression in skeletal muscle positively correlated with age and FOSL1 levels (Fig. 8 *G* and *H*). Compared to young controls, IMAT infiltration in aged human skeletal muscle was significantly increased by fourfold in paraffin sections (Fig. 8*I*), and the expression of the adipocyte marker FABP4 was significantly induced (Fig. 8*E*). Together, our results provide evidence that the FGF-2–dependent signaling pathway that causes the induction of miR-29a and the down-regulation of SPARC is conserved between mice and humans and associated with increased IMAT in human skeletal muscle.

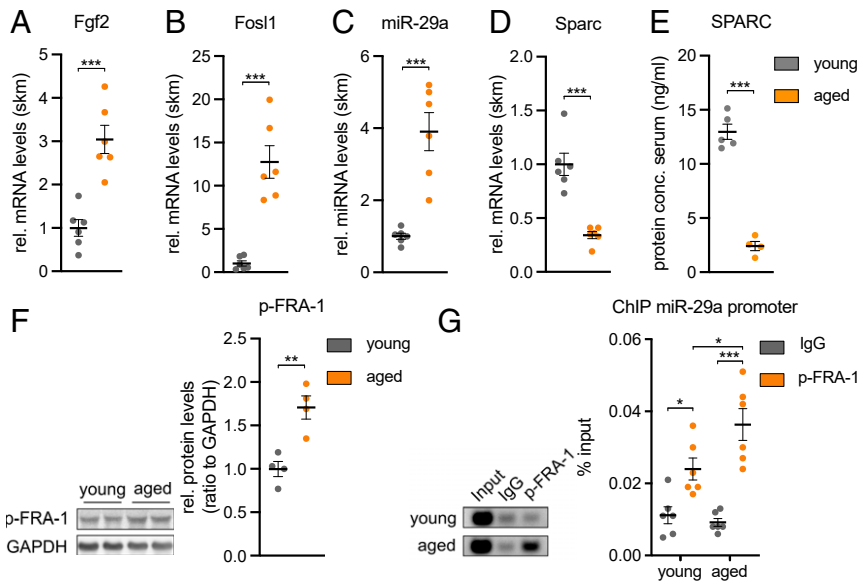


**Fig. 5.** Aged skeletal muscle contains increased p-FRA-1 levels that mediate down-regulation of Sparc by miR-29a. (*A*) Fgf2, (*B*) Fosl1, (*C*) miR-29a, and (*D*) Sparc expression in 2-mo-old (young) versus 25-mo-old (aged) mouse tibialis anterior muscle ($n = 6$). qPCR values were normalized to Tbp or snoRNA234 (miR-29a). (*E*) Levels of circulating SPARC levels in young versus aged mice as assessed by enzyme-linked immunosorbent assay ($n = 5$ versus 4). (*F*) Immunoblot depicting phosphorylation of FRA-1 in young versus aged mouse tibialis anterior muscle ($n = 4$). Band densities were quantified and normalized to GAPDH. (*G*) ChIP of p-FRA1 on miR-29a promoter performed in young versus aged mouse gastrocnemius muscle ($n = 6$). miR-29a promoter enrichment was assessed relative to total input DNA by qPCR and is depicted in relation to negative control (IgG). Representative samples were visualized on an agarose gel (*Left*). All data are plotted as mean ± SEM. Significance was evaluated by (*A–F*) two-tailed unpaired Student's *t* test and (*G*) one-way ANOVA with Tukey's multiple comparisons test. $*P \leq 0.05$; $**P \leq 0.01$; $***P \leq 0.001$.

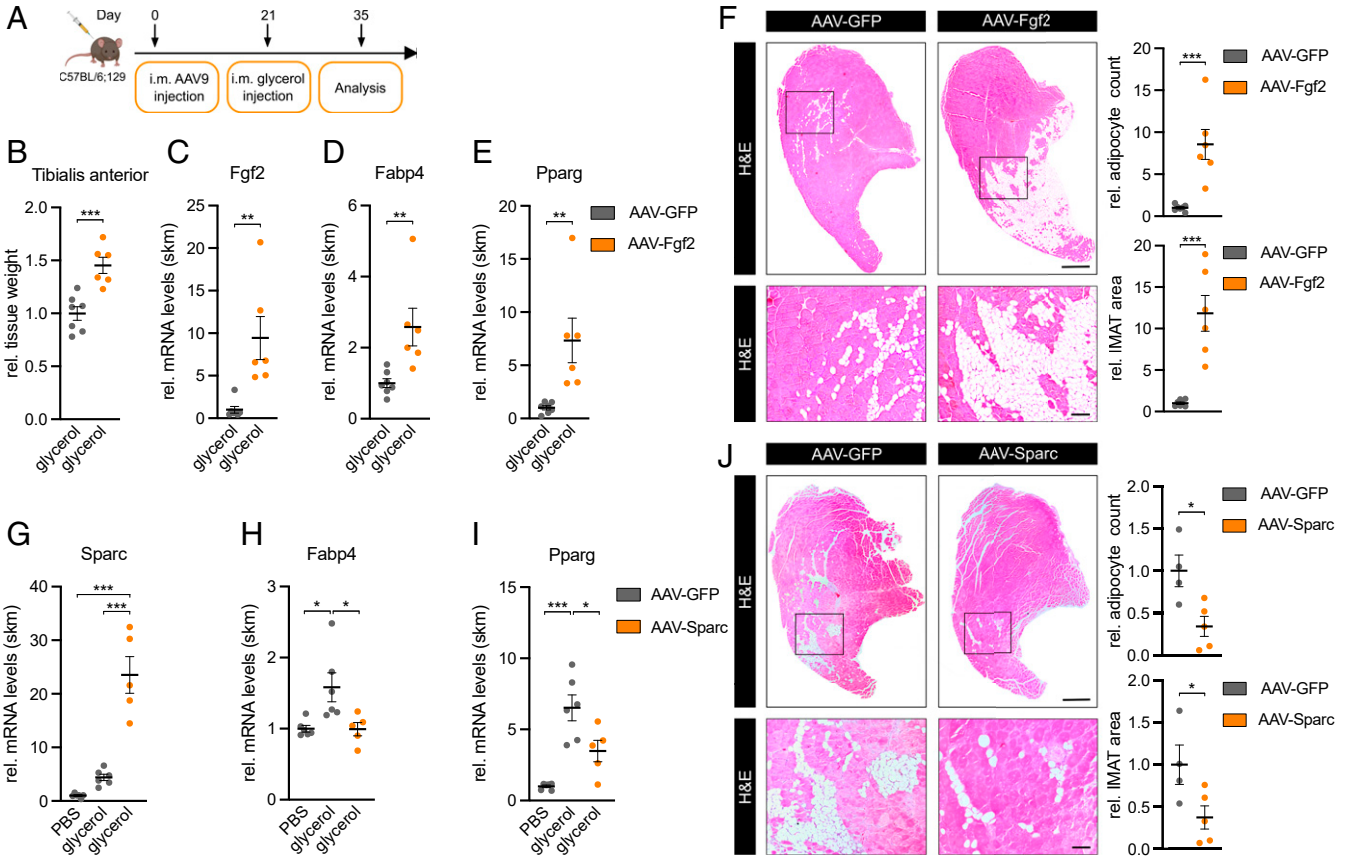


**Fig. 6.** FGF-2 and SPARC are regulators of IMAT formation. (*A*) Experimental overview of intramuscular (i.m.) AAV9 injections. (*B*) Relative tissue weight and (*C*) Fgf2, (*D*) Fabp4, and (*E*) Pparg expression in AAV-Fgf2–infected tibialis anterior muscle 2 wk after glycerol injection ($n = 7$ versus 6). qPCR values were normalized to 18S ribosomal RNA (rRNA). (*F* and *J*) IMAT formation in representative hematoxylin and eosin staining of transverse sections in (*F*) AAV-Fgf2– ($n = 7$ versus 6) or (*J*) AAV-Sparc– ($n = 4$ versus 5) infected tibialis anterior muscle 2 wk after glycerol injection and analysis of relative IMAT area and adipocyte count. (Scale bar, 0.5 mm, *Top*; 100 μm, *Bottom*.) (*G*) Sparc, (*H*) Fabp4, and (*I*) Pparg expression in AAV-Sparc–infected tibialis anterior muscle 2 wk after glycerol injection ($n = 6$ versus 6 versus 5). qPCR values were normalized to 18S rRNA. All data are plotted as mean ± SEM. Significance was evaluated by (*B–F* and *J*) two-tailed unpaired Student's *t* test and (*G–I*) one-way ANOVA with Tukey's multiple comparisons test. $^*P \leq 0.05$; $^{**}P \leq 0.01$; $^{***}P \leq 0.001$.

## Discussion

FGF-2 is a critical growth factor for myogenic progenitor cells (MPs) in the adult muscle stem cell niche. Here, we report the link between FGF-2 and IMAT formation. Our results reveal two opposing roles of FGF-2 with beneficial or adverse effects in skeletal muscle, the stimulation of muscle growth on the one hand and the increase in IMAT on the other. Targeting the adipogenic axis of FGF-2 signaling could ameliorate function and prevent adverse outcomes associated with the aged skeletal muscle.

FGF-2 signaling in human skeletal muscle is poorly understood (43). Our data provide insights into the effects of aging on FGF-2. We show that FGF-2 expression in human skeletal muscle positively correlates with aging and that aging affects miR-29a and SPARC expression, two signaling molecules downstream of FGF-2. In muscle, FGF-2 is secreted by both MPs (44) and adult myofibers (28, 45) onto the extracellular matrix of skeletal muscle (46) and predominantly affects the proliferation of MPs. In fact, the inhibition of FGF-2 signaling induced differentiation of MPs and decreased muscle mass (47). In addition, FGF-2 might promote vessel formation (48) since FGF-2 gene delivery to excisional muscle wounds enhanced not only the formation of regenerating myotubes but also angiogenesis (49). Our results identify FAPs as a third population of cells that benefit from FGF-2 during muscle injury. The role of FGF-2 signaling during adipogenesis in classical fat depots has produced conflicting results. FGF-2 enhances adipogenesis in mesenchymal stem cells (50). Additionally, the activation of p44/42 MAPK signaling initiates differentiation in preadipocytes (51), although the phosphorylation of PPAR-γ by MAPK prevents the final maturation of adipocytes (52). FGF-2 inhibited adipogenesis of human bone marrow stromal cells (53), and the disruption of FGF-2 activated the adipogenic program in mesenchymal marrow stromal cells (54). The differential effects of FGF-2 for classical WAT might reflect a concentration-dependent biphasic effect (55).

We have identified SPARC as the link between FGF-2 and IMAT formation in skeletal muscle. We use multiple strategies to demonstrate that SPARC is a direct target of miR-29a and that this relationship is conserved across species. SPARC expression is enhanced when FGF-2/MEK1/2 signaling is inhibited in both murine and human primary muscle cells. Furthermore, genomic mutations in the SPARC 3′ UTR abolish FGF-2 as well as miR-29a–mediated repression, increase SPARC secretion, and inhibit FAPs differentiation in coculture systems. Our results are in line with the role of SPARC in the classical white adipose depot in which SPARC participates in the inhibition of white adipocyte differentiation (56–58). Sparc-null mice have larger subcutanous and larger epididymal fat pads (56). SPARC is a matrix-associated glycoprotein that elicits changes in cell shape, inhibits cell-cycle progression, and influences the synthesis of extracellular matrix (56, 59). The mechanisms of SPARC involving adipogenesis include remodeling the extracellular matrix by enhancing the deposition of fibronectin and the expression of its receptor α5-integrin

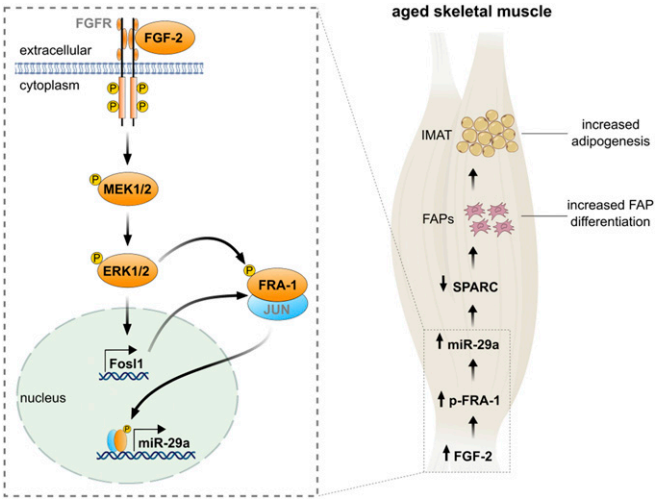


**Fig. 7.** An FGF-2 signaling pathway promotes intramuscular adipogenesis in the aged skeletal muscle. Binding of fibroblast growth factor-2 (FGF-2) phosphorylates the intracellular tyrosine kinase domain of fibroblast growth factor receptor (FGFR), which activates intracellular signaling pathways including MAPK/ERK kinase 1/2 (MEK1/2) to phosphorylate extracellular signal-regulated kinases (ERK1/2; p44/42 MAPK). MAPK activity increases both the abundance of Fosl1 and transactivating capacities of the Fos–Jun heterodimer. Phosphorylation of Fos-related antigen (FRA-1) enhances its binding to the activator protein-1 (AP-1) DNA-binding site located in the miR-29a promoter to stimulate transcription. In the aged skeletal muscle, enhanced FGF-2 signaling increases phosphorylated FRA-1 levels, which in turn promote miR-29a expression. Enhanced miR-29a levels stimulate differentiation of FAPs into adipocytes via the reduction of SPARC, promoting IMAT formation.

or inhibition of laminin expression and its α6-integrin receptor (57). Moreover, SPARC has been shown to promote the accumulation of β-catenin (57), which inhibits PPAR-γ activity (60). Interestingly, exercise stimulates SPARC expression in skeletal muscle from human and mice (23). Our data might therefore have clinical implications for strategies to prevent IMAT formation, for example, the design of exercise protocols that aim to maximize SPARC levels in muscle tissue. Mild exercise or higher intensity exercise has already been shown to increase SPARC expression in skeletal muscle in elderly individuals (61, 62). While the effects of SPARC on IMAT are striking, less is known about the effects of SPARC on muscle regeneration. After the overexpression of SPARC in skeletal muscle, we noted a small decrease in fiber number and shift to smaller fiber diameters (*SI Appendix*, Fig. S7 *A–C*), but the significance of these effects needs further investigation.

It is also important to note that not only mature myofibers but also MPs and other cell types could be an important source for SPARC in skeletal muscle. We interpret the lack of effect on Sparc mRNA in whole-muscle lysates in the Acta1-CreER model as a result of not reaching a biological threshold for the regulation of Sparc by miR-29a in myofibers. However, an alternative explanation could be that in the constitutive Pax7-Cre model, the deletion of miR-29a in MPs contributes to the increase in Sparc. Tissue panels confirm that miR-29a and Sparc are also expressed in MPs and FAPs (*SI Appendix*, Fig. S7 *D* and *E*) but to a lesser extent compared to whole-muscle tissue. In addition, we have previously reported that miR-29a represents 0.1% of all miRNAs in MPs but 0.75% of all miRNAs in tibialis anterior muscle (24, 63). These data would support the hypothesis of a miR-29a threshold for Sparc regulation in mature myofibers. In any case, regardless of the potential sources for Sparc, the up-regulation of Sparc in the Pax7-Cre model demonstrates that the myogenic lineage is an important contributor for Sparc expression in skeletal muscle.

Aging is associated with a decline in the number of MPs (64) and a loss of their ability to retain a quiescent state (28). Myofibers are the principal source of FGF-2 for the satellite cell niche. Rampant FGF-2 expression in murine myofibers implicates them as the main contributors to stem cell depletion during aging (28, 29). The reason for the increased FGF-2 in aged skeletal muscle is not known but might reflect a failed attempt to repair the aged muscle. Indeed, the activation of FGF/p38 MAPK has been demonstrated in aged satellite cells (65). Furthermore, FGF-2 target genes p21 and p16 are more epigenetically silenced in young versus old stem cells (29). FGF signaling is complex and depends on the availability of not only FGF-2 but also of coreceptors and components of the extracellular matrix such as syndecan-4, β1-integrin, and fibronectin (26, 65). Also, dynamic changes in the sulfation levels of heparin sulfate increased FGF-2 signaling in aged skeletal muscle (66). The identification of precise FGF-2 signaling events in aged skeletal muscle in our study should aid in the accurate estimation of FGF-2 signaling capacity not only during aging but also in other clinically relevant pathologies such as obesity or muscle atrophy in which FGF-2 signaling events have not been reported yet. A pronounced tissue heterogeneity might provide limitations for using a bulk analysis of FGF-2 signaling in muscle samples in vivo. While AAV-Fgf2 induced miR-29a and reduced Sparc levels as expected in primary myotubes in vitro (*SI Appendix*, Fig. S7 *F–I*), we did not observe the same correlations in our muscle samples at day 35 after AAV-Fgf2 injection (*SI Appendix*, Fig. S7 *J–L*). The massive fatty infiltration might require a better spatial resolution of gene expression analysis. Indeed, miR-29a and Sparc levels differ between muscle tissue and classical white adipose depots (*SI Appendix*, Fig. S7 *M* and *N*), while their expression in intramuscular adipocytes is still unknown.

Through classical promoter analysis experiments and bioinformatics, we identified the AP-1–binding site on the miR-29a promoter and the TF FRA-1 as effector. FRA-1 is the TF which responds to FGF-2 as well as MEK1/2 treatments. Manipulations of FGF-2/MEK1/2 resulted in regulations of FRA-1 and miR-29a. Our results provide an insight into the role of AP-1 in adult skeletal muscle. Previous studies focused on its role during muscle cell differentiation in which c-jun and MyoD can coordinate muscle enhancer factors (67), and AP-1 sites might share putative common target genes with MEF2 (68). The expression of FRA-1 is reduced during C2C12 differentiation (68) in line with the decrease in miR-29a expression (22). A role for AP-1 in adult skeletal muscle is supported by findings that the expression of AP-1 members in human skeletal muscle increases after exercise, with the highest regulation observed for FOSL1 (69). Furthermore, in a mouse model for muscle atrophy, FRA-1 binding to the MMP-2 promoter increased fourfold (70). Our results indicate that FRA-1 could be an important component of the response of skeletal muscle during aging.

Undifferentiated proliferating FAPs are necessary for successful muscle regeneration (71). Accordingly, FAPs cannot simply be erased to prevent IMAT. Therefore, strategies are needed that can modulate the fate of FAPs and their propensity to differentiate to adipocytes in disease states. The extracellular matrix (ECM) seems to be an important mediator of the cell fate of FAPs. In a mouse model of limb girdle muscular dystrophy 2B, the progressive accumulation of annexin A2 in the myofiber ECM promoted FAP differentiation into adipocytes, while a lack of annexin A2 prevented FAP adipogenesis (72). Additionally, the type 2 innate immune system has also been shown to regulate FAPs. Il4/Il13 secretion from eosinophils can activate the proliferation of FAPs, and injections of Il4 during glycerol-induced muscle regeneration reduced the formation of adipocytes (73). Targeting the fate of FAPs seems to be a promising strategy to

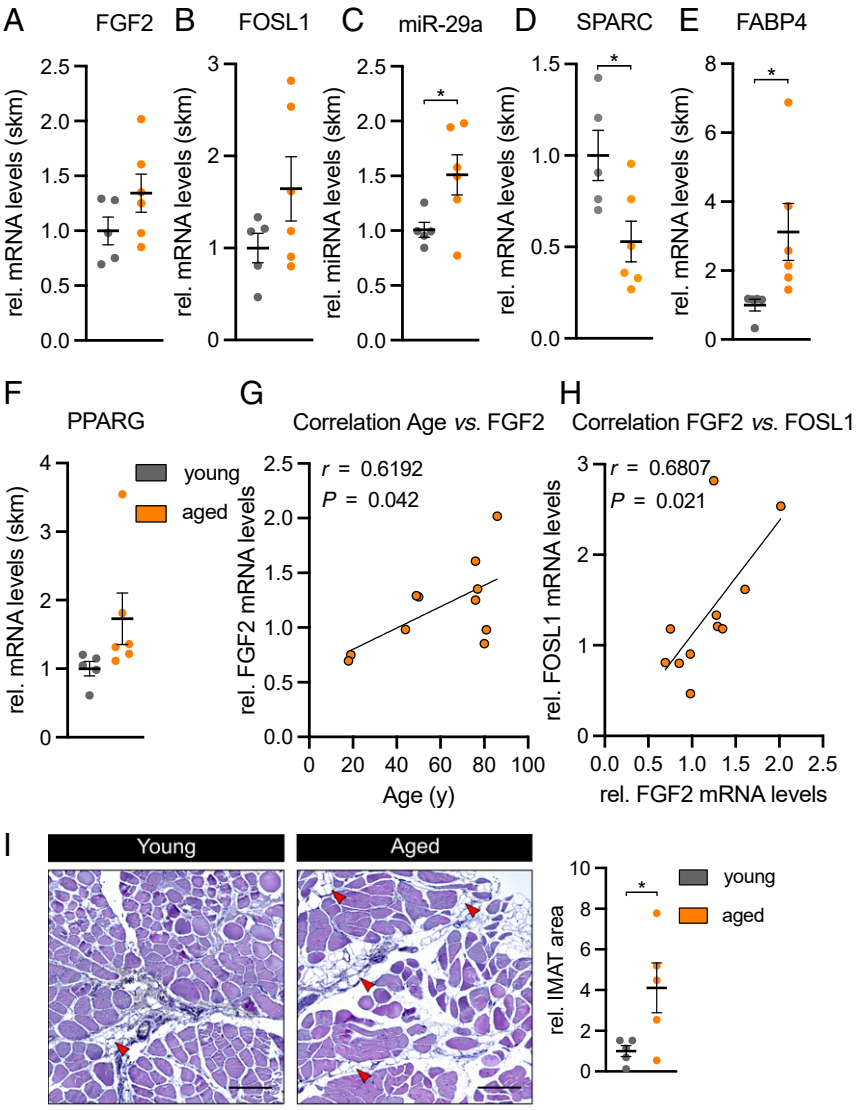


**Fig. 8.** Aged human skeletal muscle shows decreased SPARC levels and increased IMAT formation. (*A*) FGF2, (*B*) FOSL1, (*C*) miR-29a, (*D*) SPARC, (*E*) FABP4, and (*F*) PPARG expression in young (<55 y; $n = 5$) versus aged (>75 y; $n = 6$) Tensor fasciae latae muscle. qPCR values were normalized to 18S ribosomal RNA or U6 small nuclear RNA (miR-29a). (*G* and *H*) Pearson correlation and linear regression line between (*G*) age versus FGF2 mRNA expression and (*H*) FGF2 versus FOSL1 mRNA expression in Tensor fasciae latae muscle of young and aged donors ($n = 11$). (*I*) IMAT formation in representative hematoxylin and eosin stainings of transverse sections from young versus aged Tensor fasciae latae muscle. Intramuscular adipocytes are indicated by red arrowheads. (Scale bar, 200 μm.) Relative IMAT area was quantified in two consecutive sections obtained from two different areas per donor ($n = 5$). All data are plotted as mean ± SEM. Significance was evaluated by (*A*–*F* and *I*) two-tailed unpaired Student's *t* test and (*G* and *H*) Pearson correlation coefficients. *$P \leq 0.05$.

prevent IMAT formation. Secreted factors such as SPARC therefore represent important therapeutic targets.

To date, the regulation of IMAT formation is poorly understood. Linking growth factor signaling pathways to the pleiotropic effects of miRNAs to myokine secretion and FAP differentiation has the potential to provide novel diagnostic and therapeutic approaches. Early detection of an increased risk for IMAT based on the FGF-2/FRA-1/miR-29a/SPARC axis and its use to improve fatty muscle degeneration could help to prevent IMAT and its sequelae, loss of muscle mass, and function in the older population.

## Materials and Methods

Details of human patients and the full procedures for animal experiments, cell preparation, fluorescence-activated cell sorting, cell culture, RNA extraction, complementary DNA synthesis, qRT-PCR, proliferation assay, enzyme-linked immunosorbent assay, plasmid construction, luciferase assay, CRISPR-Cas9 genome editing, AAV production, ChIP, protein extraction, Western blot, histology, LC-MS/MS, RNA sequencing, bioinformatics, and statistical analysis are provided in *SI Appendix*.

**Data Availability.** We declare that all data supporting the findings of this study are available within the article and its *SI Appendix* and have been deposited in Dryad (DOI: 10.5061/dryad.j6q573nf6) (74). The RNA sequencing data described in this report have been deposited in the Gene Expression Omnibus database (GSE154254) (75). The mass spectrometry proteomics data have been deposited to the ProteomeXchange consortium via the Proteomics Identifications Database (PRIDE) partner repository with the dataset identifier PXD020575 (76).

**ACKNOWLEDGMENTS.** This study was supported by a grant from the Swiss NSF (182716) to J.K. and unrestricted grants from the Vontobel, Philhuman, Heuberg, and Uniscientia foundations to J.K. We thank Dr. Edlira Luca for the critical reading of the manuscript. We also thank the Functional Genomics Center Zurich, the Flow Cytometry Facility Zurich, and members of the Wolfrum Lab for their technical support.

1. J. Myers *et al*., Exercise capacity and mortality among men referred for exercise testing. *N. Engl. J. Med.* **346**, 793–801 (2002).
2. G. I. Shulman, Ectopic fat in insulin resistance, dyslipidemia, and cardiometabolic disease. *N. Engl. J. Med.* **371**, 1131–1141 (2014).
3. F. Zurlo, K. Larson, C. Bogardus, E. Ravussin, Skeletal muscle metabolism is a major determinant of resting energy expenditure. *J. Clin. Invest.* **86**, 1423–1427 (1990).
4. E. Goldhammer *et al*., Exercise training modulates cytokines activity in coronary heart disease patients. *Int. J. Cardiol.* **100**, 93–99 (2005).
5. F. B. Benatti, B. K. Pedersen, Exercise as an anti-inflammatory therapy for rheumatic diseases-myokine regulation. *Nat. Rev. Rheumatol.* **11**, 86–97 (2015).
6. I. H. Rosenberg, Sarcopenia: Origins and clinical relevance. *J. Nutr.* **127**, 990S–991S (1997).
7. R. N. Baumgartner *et al*., Epidemiology of sarcopenia among the elderly in New Mexico. *Am. J. Epidemiol.* **147**, 755–763 (1998).
8. S. Wild, G. Roglic, A. Green, R. Sicree, H. King, Global prevalence of diabetes: Estimates for the year 2000 and projections for 2030. *Diabetes Care* **27**, 1047–1053 (2004).
9. J. Mesinovic, A. Zengin, B. De Courten, P. R. Ebeling, D. Scott, Sarcopenia and type 2 diabetes mellitus: A bidirectional relationship. *Diabetes Metab. Syndr. Obes.* **12**, 1057–1072 (2019).
10. S. Perkisas, A. M. De Cock, V. Verhoeven, M. Vandewoude, Intramuscular adipose tissue and the functional components of sarcopenia in hospitalized geriatric patients. *Geriatrics (Basel)* **2**, 11 (2017).
11. M. Boettcher *et al*., Intermuscular adipose tissue (IMAT): Association with other adipose tissue compartments and insulin sensitivity. *J. Magn. Reson. Imaging* **29**, 1340–1345 (2009).
12. D. C. Bittel *et al*., Adipose tissue content, muscle performance and physical function in obese adults with type 2 diabetes mellitus and peripheral neuropathy. *J. Diabetes Complications* **29**, 250–257 (2015).
13. B. H. Goodpaster, F. L. Thaete, D. E. Kelley, Thigh adipose tissue distribution is associated with insulin resistance in obesity and in type 2 diabetes mellitus. *Am. J. Clin. Nutr.* **71**, 885–892 (2000).
14. T. Baum *et al*., Association of quadriceps muscle fat with isometric strength measurements in healthy males using chemical shift encoding-based water-fat magnetic resonance imaging. *J. Comput. Assist. Tomogr.* **40**, 447–451 (2016).
15. K. M. Beavers *et al*., Associations between body composition and gait-speed decline: Results from the health, aging, and body composition study. *Am. J. Clin. Nutr.* **97**, 552–560 (2013).
16. R. L. Marcus *et al*., Intramuscular adipose tissue, sarcopenia, and mobility function in older individuals. *J. Aging Res.* **2012**, 629637 (2012).
17. R. A. Murphy *et al*., Associations of BMI and adipose tissue area and density with incident mobility limitation and poor performance in older adults. *Am. J. Clin. Nutr.* **99**, 1059–1065 (2014).
18. A. W. Joe *et al*., Muscle injury activates resident fibro/adipogenic progenitors that facilitate myogenesis. *Nat. Cell Biol.* **12**, 153–163 (2010).
19. A. Uezumi, S. Fukada, N. Yamamoto, S. Takeda, K. Tsuchida, Mesenchymal progenitors distinct from satellite cells contribute to ectopic fat cell formation in skeletal muscle. *Nat. Cell Biol.* **12**, 143–152 (2010).
20. T. Gorski, S. Mathes, J. Krützfeldt, Uncoupling protein 1 expression in adipocytes derived from skeletal muscle fibro/adipogenic progenitors is under genetic and hormonal control. *J. Cachexia Sarcopenia Muscle* **9**, 384–399 (2018).
21. E. Luca *et al*., Genetic deletion of microRNA biogenesis in muscle cells reveals a hierarchical non-clustered network that controls focal adhesion signaling during muscle regeneration. *Mol. Metab.* **36**, 100967 (2020).
22. A. Galimov *et al*., MicroRNA-29a in adult muscle stem cells controls skeletal muscle regeneration during injury and exercise downstream of fibroblast growth factor-2. *Stem Cells* **34**, 768–780 (2016).
23. W. Aoi *et al*., A novel myokine, secreted protein acidic and rich in cysteine (SPARC), suppresses colon tumorigenesis via regular exercise. *Gut* **62**, 882–889 (2013).
24. A. Galimov *et al*., Growth hormone replacement therapy regulates microRNA-29a and targets involved in insulin resistance. *J. Mol. Med. (Berl.)* **93**, 1369–1379 (2015).
25. J. L. Mott *et al*., Transcriptional suppression of mir-29b-1/mir-29a promoter by c-Myc, hedgehog, and NF-kappaB. *J. Cell. Biochem.* **110**, 1155–1164 (2010).
26. B. Pawlikowski, T. O. Vogler, K. Gadek, B. B. Olwin, Regulation of skeletal muscle stem cells by fibroblast growth factors. *Dev. Dyn.* **246**, 359–367 (2017).
27. H. Gazon, B. Barbeau, J. M. Mesnard, J. M. Peloponese Jr, Hijacking of the AP-1 signaling pathway during development of ATL. *Front. Microbiol.* **8**, 2686 (2018).
28. J. V. Chakkalakal, K. M. Jones, M. A. Basson, A. S. Brack, The aged niche disrupts muscle stem cell quiescence. *Nature* **490**, 355–360 (2012).
29. J. Li, S. Han, W. Cousin, I. M. Conboy, Age-specific functional epigenetic changes in p21 and p16 in injury-activated satellite cells. *Stem Cells* **33**, 951–961 (2015).
30. P. V. Sepulveda *et al*., Evaluation of follistatin as a therapeutic in models of skeletal muscle atrophy associated with denervation and tenotomy. *Sci. Rep.* **5**, 17535 (2015).
31. Y. Guo *et al*., AMP-activated kinase α2 deficiency protects mice from denervation-induced skeletal muscle atrophy. *Arch. Biochem. Biophys.* **600**, 56–60 (2016).
32. C. W. Baumann, H. M. Liu, L. V. Thompson, Denervation-induced activation of the ubiquitin-proteasome system reduces skeletal muscle quantity not quality. *PLoS One* **11**, e0160839 (2016).
33. S. D. Kunkel *et al*., mRNA expression signatures of human skeletal muscle atrophy identify a natural compound that increases muscle mass. *Cell Metab.* **13**, 627–638 (2011).
34. G. Zhang *et al*., Toll-like receptor 4 mediates Lewis lung carcinoma-induced muscle wasting via coordinate activation of protein degradation pathways. *Sci. Rep.* **7**, 2273 (2017).
35. D. E. Lee *et al*., Cancer cachexia-induced muscle atrophy: Evidence for alterations in microRNAs important for muscle size. *Physiol. Genomics* **49**, 253–260 (2017).
36. S. Liu *et al*., L-carnitine ameliorates cancer cachexia in mice by regulating the expression and activity of carnitine palmityl transferase. *Cancer Biol. Ther.* **12**, 125–130 (2011).
37. M. Petruzzelli *et al*., A switch from white to brown fat increases energy expenditure in cancer-associated cachexia. *Cell Metab.* **20**, 433–447 (2014).
38. M. Isotani, K. Miyake, N. Miyake, Y. Hirai, T. Shimada, Direct comparison of four adeno-associated virus serotypes in mediating the production of antiangiogenic proteins in mouse muscle. *Cancer Invest.* **29**, 353–359 (2011).
39. J. P. Louboutin, L. Wang, J. M. Wilson, Gene transfer into skeletal muscle using novel AAV serotypes. *J. Gene Med.* **7**, 442–451 (2005).
40. M. Tabebordbar *et al*., In vivo gene editing in dystrophic mouse muscle and muscle stem cells. *Science* **351**, 407–411 (2016).
41. M. Riaz *et al*., Differential myofiber-type transduction preference of adeno-associated virus serotypes 6 and 9. *Skelet. Muscle* **5**, 37 (2015).
42. L. Muraine *et al*., Transduction efficiency of AAV serotypes after local injection in mouse and human skeletal muscle. *Hum. Gene Ther.* **31**, 233–240 (2019).
43. H. Ghanim *et al*., Effect of testosterone on FGF2, MRF4, and myostatin in hypogonadotropic hypogonadism: Relevance to muscle growth. *J. Clin. Endocrinol. Metab.* **104**, 2094–2102 (2019).
44. K. Hannon, A. J. Kudla, M. J. McAvoy, K. L. Clase, B. B. Olwin, Differentially expressed fibroblast growth factors regulate skeletal muscle development through autocrine and paracrine mechanisms. *J. Cell Biol.* **132**, 1151–1159 (1996).
45. J. E. Anderson, C. M. Mitchell, J. K. McGeachie, M. D. Grounds, The time course of basic fibroblast growth factor expression in crush-injured skeletal muscles of SJL/J and BALB/c mice. *Exp. Cell Res.* **216**, 325–334 (1995).
46. J. DiMario, N. Buffinger, S. Yamada, R. C. Strohman, Fibroblast growth factor in the extracellular matrix of dystrophic (mdx) mouse muscle. *Science* **244**, 688–690 (1989).
47. H. Flanagan-Steet, K. Hannon, M. J. McAvoy, R. Hullinger, B. B. Olwin, Loss of FGF receptor 1 signaling reduces skeletal muscle mass and disrupts myofiber organization in the developing limb. *Dev. Biol.* **218**, 21–37 (2000).
48. I. Stratos *et al*., Fibroblast growth factor-2-overexpressing myoblasts encapsulated in alginate spheres increase proliferation, reduce apoptosis, induce adipogenesis, and enhance regeneration following skeletal muscle injury in rats. *Tissue Eng. Part A* **17**, 2867–2877 (2011).
49. J. Doukas *et al*., Delivery of FGF genes to wound repair cells enhances arteriogenesis and myogenesis in skeletal muscle. *Mol. Ther.* **5**, 517–527 (2002).
50. M. Neubauer *et al*., Basic fibroblast growth factor enhances PPARgamma ligand-induced adipogenesis of mesenchymal stem cells. *FEBS Lett.* **577**, 277–283 (2004).
51. D. Prusty, B. H. Park, K. E. Davis, S. R. Farmer, Activation of MEK/ERK signaling promotes adipogenesis by enhancing peroxisome proliferator-activated receptor gamma (PPARgamma) and C/EBPalpha gene expression during the differentiation of 3T3-L1 preadipocytes. *J. Biol. Chem.* **277**, 46226–46232 (2002).
52. H. S. Camp, S. R. Tafuri, Regulation of peroxisome proliferator-activated receptor gamma activity by mitogen-activated protein kinase. *J. Biol. Chem.* **272**, 10811–10816 (1997).
53. S. Le Blanc, M. Simann, F. Jakob, N. Schütze, T. Schilling, Fibroblast growth factors 1 and 2 inhibit adipogenesis of human bone marrow stromal cells in 3D collagen gels. *Exp. Cell Res.* **338**, 136–148 (2015).
54. L. Xiao *et al*., Disruption of the Fgf2 gene activates the adipogenic and suppresses the osteogenic program in mesenchymal marrow stromal stem cells. *Bone* **47**, 360–370 (2010).
55. S. Kim, C. Ahn, N. Bong, S. Choe, D. K. Lee, Biphasic effects of FGF2 on adipogenesis. *PLoS One* **10**, e0120073 (2015).
56. A. D. Bradshaw, D. C. Graves, K. Motamed, E. H. Sage, SPARC-null mice exhibit increased adiposity without significant differences in overall body weight. *Proc. Natl. Acad. Sci. U.S.A.* **100**, 6045–6050 (2003).
57. J. Nie, E. H. Sage, SPARC inhibits adipogenesis by its enhancement of beta-catenin signaling. *J. Biol. Chem.* **284**, 1279–1290 (2009).
58. T. D. Challa *et al*., Regulation of de novo adipocyte differentiation through cross talk between adipocytes and preadipocytes. *Diabetes* **64**, 4075–4087 (2015).
59. E. Hohenester, T. Sasaki, C. Giudici, R. W. Farndale, H. P. Bächinger, Structural basis of sequence-specific collagen recognition by SPARC. *Proc. Natl. Acad. Sci. U.S.A.* **105**, 18273–18277 (2008).
60. J. Liu, H. Wang, Y. Zuo, S. R. Farmer, Functional interaction between peroxisome proliferator-activated receptor gamma and beta-catenin. *Mol. Cell. Biol.* **26**, 5827–5837 (2006).
61. I. Riedl *et al*., Regulation of skeletal muscle transcriptome in elderly men after 6 weeks of endurance training at lactate threshold intensity. *Exp. Gerontol.* **45**, 896–903 (2010).
62. S. Radom-Aizik *et al*., Effects of aerobic training on gene expression in skeletal muscle of elderly men. *Med. Sci. Sports Exerc.* **37**, 1680–1696 (2005).
63. A. Mizbani, E. Luca, E. J. Rushing, J. Krützfeldt, MicroRNA deep sequencing in two adult stem cell populations identifies miR-501 as a novel regulator of myosin heavy chain during muscle regeneration. *Development* **143**, 4137–4148 (2016).
64. G. Shefer, D. P. Van de Mark, J. B. Richardson, Z. Yablonka-Reuveni, Satellite-cell pool size does matter: Defining the myogenic potency of aging skeletal muscle. *Dev. Biol.* **294**, 50–66 (2006).
65. J. D. Bernet *et al*., p38 MAPK signaling underlies a cell-autonomous loss of stem cell self-renewal in skeletal muscle of aged mice. *Nat. Med.* **20**, 265–271 (2014).
66. R. S. Ghadiali, S. E. Guimond, J. E. Turnbull, A. Pisconti, Dynamic changes in heparan sulfate during muscle differentiation and ageing regulate myoblast cell fate and FGF2 signalling. *Matrix Biol.* **59**, 54–68 (2017).
67. R. Blum, V. Vethantham, C. Bowman, M. Rudnicki, B. D. Dynlacht, Genome-wide identification of enhancers in skeletal muscle: The role of MyoD1. *Genes Dev.* **26**, 2763–2779 (2012).

68. S. W. Tobin *et al*., Regulation of Hspb7 by MEF2 and AP-1: Implications for Hspb7 in muscle atrophy. *J. Cell Sci.* **129**, 4076–4090 (2016).
69. A. Puntschart *et al*., Expression of fos and jun genes in human skeletal muscle after exercise. *Am. J. Physiol.* **274**, C129–C137 (1998).
70. X. Liu, G. Manzano, D. H. Lovett, H. T. Kim, Role of AP-1 and RE-1 binding sites in matrix metalloproteinase-2 transcriptional regulation in skeletal muscle atrophy. *Biochem. Biophys. Res. Commun.* **396**, 219–223 (2010).
71. M. N. Wosczyna *et al*., Mesenchymal stromal cells are required for regeneration and homeostatic maintenance of skeletal muscle. *Cell Rep.* **27**, 2029–2035.e5 (2019).
72. M. W. Hogarth *et al*., Fibroadipogenic progenitors are responsible for muscle loss in limb girdle muscular dystrophy 2B. *Nat. Commun.* **10**, 2430 (2019).
73. J. E. Heredia *et al*., Type 2 innate signals stimulate fibro/adipogenic progenitors to facilitate muscle regeneration. *Cell* **153**, 376–388 (2013).
74. S. Mathes *et al*., FGF-2-dependent signaling activated in aged skeletal muscle promotes intramuscular adipogenesis. *Dryad*. https://datadryad.org/stash/dataset/doi:10.5061/dryad.j6q573nf6. Deposited 17 July 2021.
75. E. Luca, A. Hartung, S. Mathes, H. Rehrauer, J. Krützfeldt, Genetic deletion of microRNA biogenesis in muscle cells reveals a hierarchical non- clustered network that controls focal adhesion signaling during muscle regeneration. *Gene Expression Omnibus*. https://www.ncbi.nlm.nih.gov/geo/query/acc.cgi?acc=GSE154254. Deposited 11 July 2020.
76. S. Mathes, J. Krützfeldt, An FGF-2 signaling pathway that is activated in aged skeletal muscle promotes intramuscular adipogenesis. Proteomics Identifications Database (PRIDE). http://www.ebi.ac.uk/pride/archive/projects/PXD020575. Deposited 27 July 2020.